Photocarrier dynamics in anatase TiO_2: Evidence of thermally activated collisions between carriers

Adrien Girault,[1,2,3] Mathieu Gallart,[1] Marc Ziegler,[1] Olivier Crégut,[1] Matteo Balestrieri,[3] Iryna Gozhyk,[3] Hervé Montigaud,[3] Davide Sciacca,[2] Lorenzo Mancini,[2] and Pierre Gilliot[1,*]

[1]*IPCMS UMR 7504, CNRS, Université de Strasbourg, 23 rue du Læss, Boîte Postale 43, F-67034 Strasbourg CEDEX 2, France*

[2]*Saint-Gobain Research Paris, 39 quai Lucien Lefranc, F-93303 Aubervilliers CEDEX, France*

[3]*Laboratoire "Surface du Verre et Interfaces" UMR 125 Saint-Gobain, CNRS, 39 quai Lucien Lefranc, F-93303 Aubervilliers CEDEX, France*

(Received 17 May 2023; accepted 11 October 2023; published 25 October 2023)

The photoluminescence emission spectrum at low temperature of the TiO_2 anatase shows a broad band around 2.3 eV that has been largely attributed to self-trapped excitons. In this paper, time-resolved experiments conducted at low temperature on a thin layer and a single crystal give insights into the carrier dynamics inside TiO_2. The decay of the photoluminescence with time can be described by a single power law from the picoseconds time range up to the milliseconds time range. The decay rate increases with increasing temperature. We propose to interpret these observations by a collision mechanism between self-trapped excitons that diffuse via hopping processes. These excitons, which are stabilized by the indirect band gap of anatase TiO_2, can be ionized at higher temperatures and lead thus to an acceleration of the observed dynamics.

DOI: 10.1103/PhysRevB.108.155204

I. INTRODUCTION

Titanium dioxide (TiO_2) is a semiconductor known for its photocatalytic activity and its ability to transport carriers [1]. It is known as nontoxic, resilient, and abundant and is thus widely used in photoconversion applications [1]. TiO_2 can be found in two main crystalline forms, rutile and anatase, that are stable at ambient temperature. Both phases have been widely studied for photovoltaics, especially after the creation of the first dye-sensitized solar cell by Grätzel in 1991 [2,3]. For photocatalytic application, the most interesting phase is anatase due to its higher photoconversion efficiency as compared with rutile [4]. This phase is organized in TiO_6 octahedra [1] and presents an optical gap of 3.31 eV [5]. The photocatalytic properties come from the photogeneration, within the material, of charge carriers, electrons (e) and holes (h), that will diffuse towards the surface where they become available for redox reactions. Therefore most photocatalytic applications of TiO_2 use nanoparticles for which the surface-to-volume ratio is important. Another possibility is to use thin layers (∼10–20 nm) deposited on the surface of another material. This configuration avoids the creation of TiO_2 nanoparticles.

The photocatalytic properties are intimately related to the optoelectronic behavior of TiO_2. Several studies were conducted in the 1980s [6,7] to get a better comprehension of the excitonic states in various TiO_2 polymorphs including rutile and $SrTiO_3$. The optoelectronic properties of $SrTiO_3$ are very close to those of anatase TiO_2. The first extensive studies on the photoluminescence of anatase were performed by Tang *et al.* [8,9]. The experiments showed an absorption in the near-UV range and a broad photoluminescence in the visible spectral range (very large Stokes shift) at low temperature that is usually explained by the formation of self-trapped excitons (STEs). Analysis of the Urbach tail gave more hints about the presence of STEs. Hosaka *et al.* [10] also studied the photoluminescence of TiO_2 and its dependence on the polarization of the excitation light proving that the luminescence is not due to defects but is intrinsic to the material. Finally, the dependence with temperature of the luminescence has been studied by Bieber *et al.* [11] and Gallart *et al.* [12]. The decrease of the photoluminescence intensity with temperature has been interpreted using a four-energy-level model that explains the hopping of the carriers to surface states and the quenching of the luminescence. The carriers in TiO_2 can then be considered as polarons that interact weakly with each other but are strongly bound to the lattice. This model has been successfully used by Bégin-Colin *et al.* [13] to link this four-level model to the photoactivity of various commercial powders of anatase.

Time-resolved experiments have also been reported [14,15]. An extremely long dynamics was evidenced and confirmed in other papers [16,17]. The fit of the data was made either by a double exponential [18] or by a combination of an exponential and an empirical power function [14,15]. The decay of the photoluminescence in anatase has then been explained by two different STE formation paths.

In spite of this abundant literature, the exact nature of carriers in anatase TiO_2 is still unclear, the respective roles of free carriers, free excitons, polarons, and STE states remain ambiguous, and many interpretations are offered in recent reviews [1,5,19–21]. In this regard, this paper is based on a comprehensive experimental study of the photoluminescence time decay and aims at bringing a clarified understanding of the experimental data.

II. SAMPLES AND EXPERIMENTAL SETUPS

A. Anatase samples

We used two types of anatase samples. The first one is a commercial single crystal presenting a surface with 110

*pierre.gilliot@ipcms.unistra.fr

orientation (Surface Preparation Laboratory, Wormerveer, The Netherlands), referred to as the A110 sample in the following. The second one is a thin (80 nm) layer that was deposited on commercial glass via magnetron sputtering using an under-stoichiometric TiO_2 target. The deposition was performed in the presence of oxygen. A thermal activation is needed for crystallization to occur. This thermal activation was performed at 650 °C during 10 min in an industrial oven. This sample will be referred to as the magnetron sample.

B. Temperature-dependent photoluminescence measurements

Photoluminescence (PL) experiments have been conducted at different temperatures using a Cryo Industries cryostat where the sample was fixed to a cold finger by a silver paste. The explored temperature range goes down to 10 K. The excitation source was a LASOS single-frequency diode-pumped solid state laser emitting in the UV range at 320 nm. The PL emission was spectrally resolved using a SPEX 270M spectrometer and recorded using a liquid-nitrogen-cooled CCD camera.

A white-light lamp coupled to a monochromator allowed us to tune the excitation wavelength and record the PL excitation spectra (300–400 nm).

C. Time-resolved photoluminescence measurements: Streak camera

Time-resolved photoluminescence experiments were carried out from room temperature down to 10 K using an Oxford Instruments cryostat. As before, the sample was fixed to the cold finger. The excitation source comes from a 1030-nm pulsed ytterbium laser (Tangerine laser from Amplitude). Mixing the second harmonic with a continuum generates 320-nm pulses with a duration of 270 fs. The repetition rate is adjustable between 1 and 100 kHz. The detection setup consists of a spectrometer paired with a Hamamatsu streak camera (C10627) synchronized with the excitation pulse. The acquisitions were made in photon-counting mode.

III. RESULTS

A. Photoluminescence excitation

Let us start by describing the photoluminescence excitation (PLE) spectra of the two samples. The maximum of emission occurs at an excitation of 3.4 eV (365 nm) for the single crystal (Fig. 1) as expected from the literature [11,12,22]. The maximum of the thin layers is deeper in the UV range (Fig. 2) at 3.9 eV (320 nm). This band-gap increase can be explained by confinement effects.

The emission band is nearly the same for both samples. It is characterized by a very broad emission band with a maximum of 2.4 eV. This emission band is asymmetric: A fit by at least two Gaussian peaks is needed to get a good agreement with the experimental data. The PLE spectra show a large difference of nearly 1.1–1.5 eV between the excitation and the emission energies (large Stokes shift), a fact that is usually related to the formation of STEs.

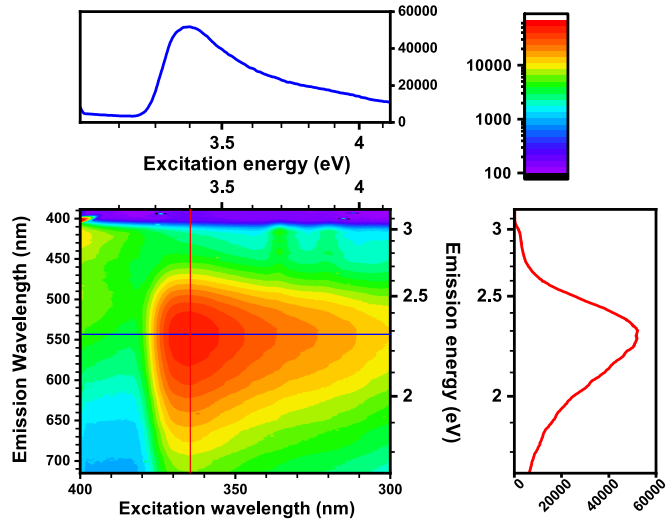

FIG. 1. Low-temperature ($T = 10$ K) PLE map of the A110 sample. The top and right graphs are an excitation spectrum (fixed emission at 2.28 eV) and a PL spectrum (fixed excitation at 3.4 eV), respectively.

B. Temperature-dependent photoluminescence

Measurements of the PL intensity as a function of temperature were performed on the thin layers (the magnetron sample) and the single crystal (the A110 sample). The photoluminescence of the samples decreases significantly with temperature as seen in Fig. 3. This is described in Ref. [12] by a four-level model that includes thermally activated dark states. The spatial separation of carriers would thus be thermally activated, and these carriers could then be transferred to distant sites at the surface where they will be involved in redox reactions: This explains the photocatalytic activity of such samples. This will be discussed in the following.

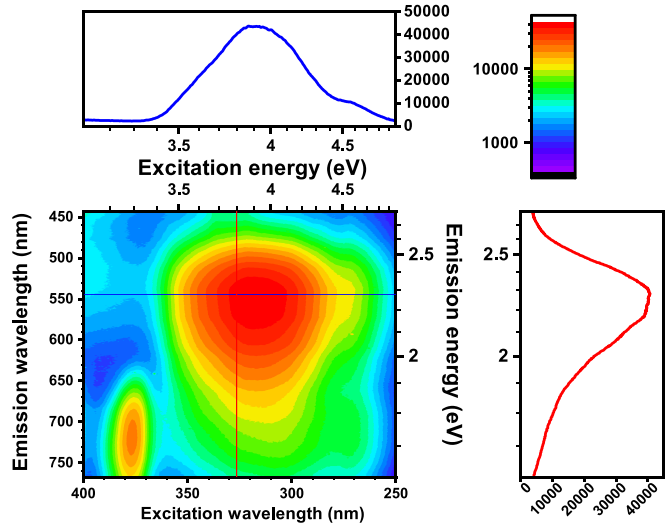

FIG. 2. Low-temperature ($T = 10$ K) PLE map of the magnetron anatase sample. The top and right graphs are an excitation spectrum (fixed emission at 2.28 eV) and a PL spectrum (fixed excitation at 3.8 eV), respectively.

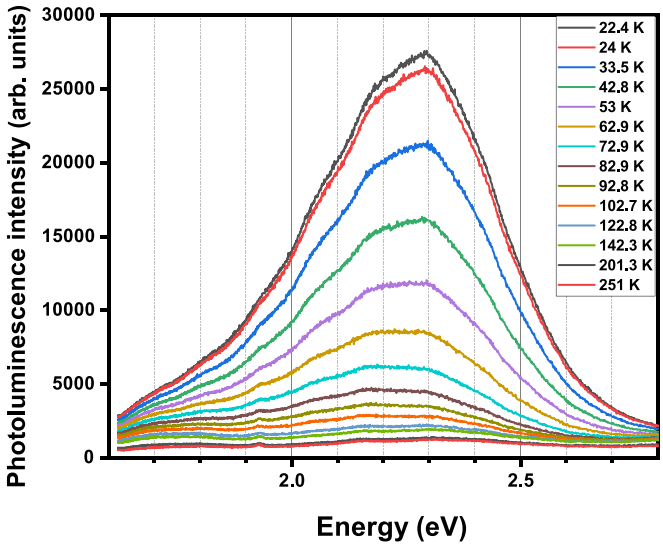

FIG. 3. Temperature decrease of the PL intensity emitted by the magnetron sample between 22 and 251 K.

C. Time-resolved photoluminescence

Time-resolved photoluminescence (TR-PL) measurements were performed on the single-crystal sample and the magnetron sample at 10 K. As shown in Figs. 4 and 5, the obtained data can be plotted on a two-dimensional (2D) map. The abscissa is the wavelength of the detected light. The ordinate is the time scale. Various time resolutions can be attained with the streak camera. Here, in Figs. 4(a) and 4(b), the time resolution is 42 ps (240 pixels in 10 ns) and 4.2 ns (240 pixels in 1 µs), respectively.

The two samples are showing a long-lived broad emission between 450 and 580 nm. This emission is comparable to what has been previously observed in the literature [15–17] and in our static experiment as well. It is characterized by a long lifetime: Photoluminescence can still be observed several microseconds after the arrival of the laser pulse.

The decay of the photoluminescence with time can be analyzed by integrating the pulse intensity over the whole emission band and at different time ranges of the streak camera. The PL intensities have been further renormalized with regard to their respective time ranges: considering, for example, that 1 pixel in the 10-ns time range merges the same number of photons as 10 pixels in the 1-ns time range. The PL intensity plotted on the y axis is thus, in arbitrary units, the value per time unit. Furthermore, as the log-log-scale representation must not suffer any axis shift, we determine precisely the time origin by fitting the TR-PL rise by a Gaussian function and taking the position of its maximum as zero time. This procedure allows us to superimpose all the data measured over different time ranges, as shown in Figs. 6 and 7.

1. Low-temperature experiments

The decays at a temperature of 10 K are shown in Fig. 6 for both samples. The different data acquired for each range of the streak camera adjust nicely into a curve that covers nearly four orders of magnitude on the signal intensity and six orders on

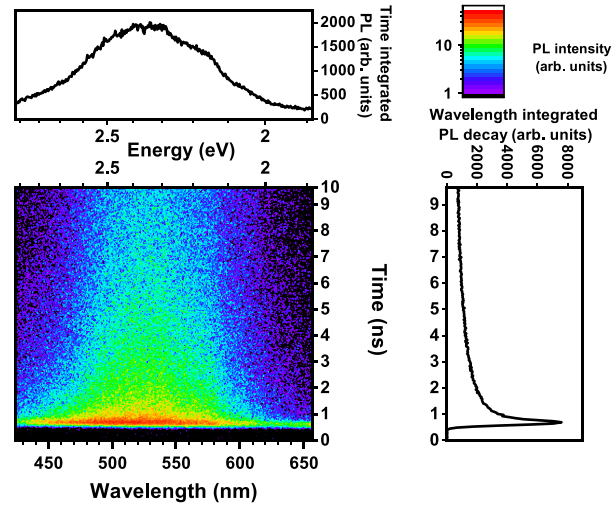

(a) 10 ns

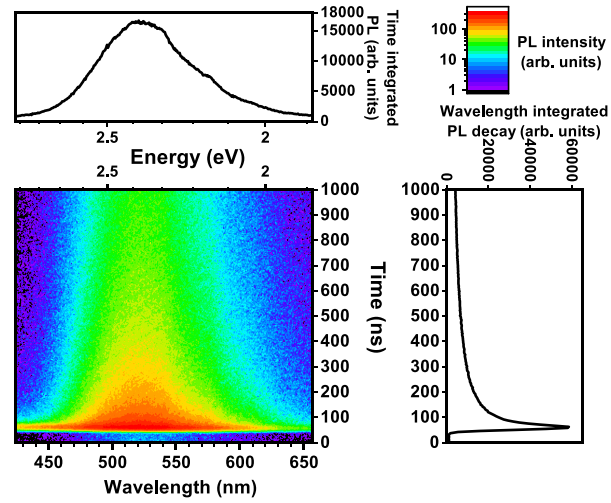

(b) 1 µs

FIG. 4. TR-PL measured on the single crystal (the A110 sample) at 10 K for two different time ranges of the streak camera: (a) 10 ns and (b) 1 µs.

the time delay. With the log-log scale that is used, the curve becomes nearly linear for times longer than 1 ns, with a slope around −0.8 for the magnetron sample and around −0.6 for the A110 sample, showing that the emission dynamics can be described by a single power law with only three parameters (see below). The curvature at shorter time delays fits also well with such a power law with no need for adding an exponential decay (see discussion below) as shown in Fig. 7.

2. Variation of the TR-PL curves with temperature

Figure 7 shows the evolution of the TR-PL intensity at various temperatures for the magnetron sample. As expected from the static temperature dependence of the photoluminescence, the increase in temperature drives a decrease in the photoluminescence intensity. A comparison between the integrated time-resolved curves and the static ones in Fig. 8 shows a correlation between the two sets of data. It is reasonable to think that the observations in both the static and time-resolved

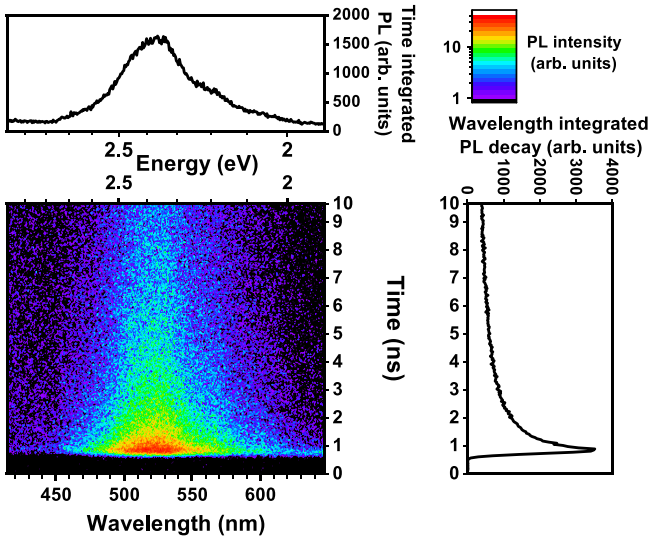

(a) 10 ns

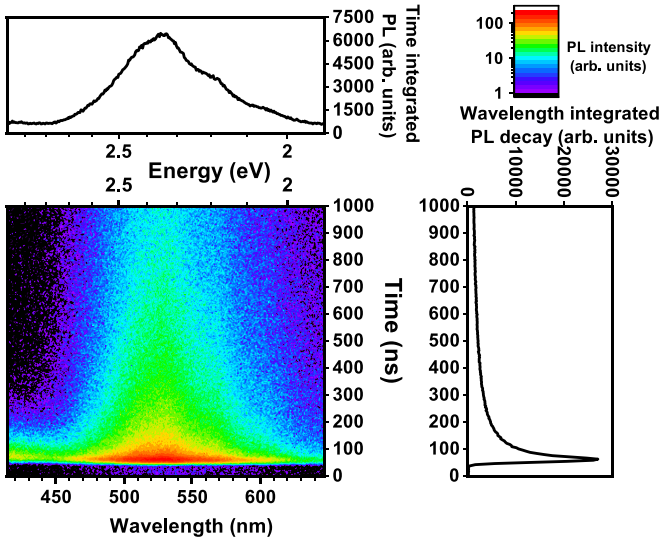

(b) 1 µs

FIG. 5. TR-PL measured on the magnetron sample at 10 K for two different time ranges of the streak camera: (a) 10 ns and (b) 1 µs.

experiments are the consequence of the same temperature-dependent mechanism.

IV. DISCUSSION

The usual emission spectrum features of TiO_2 anatase are observed in the thin-layer sample and in the bulk sample as shown in Fig. 2. No notable difference can be seen between the PL emission data of the two samples, and the changes in the PLE spectra can be attributed to the confinement effect, as a decrease in the domain size can give rise to a blueshift of the transitions. The visible broad emission band with a large Stokes shift has been attributed in the literature to different recombination mechanisms including oxygen vacancies or surface states [8,14,15,23]. However, the most commonly cited mechanism is the formation of a self-trapped exciton [9,10,23]. The creation of the STE comes from two different

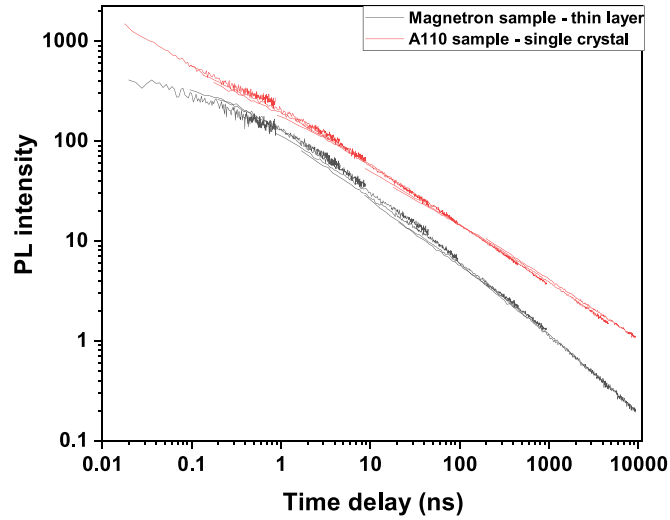

FIG. 6. PL decay of the two samples (the magnetron sample and the A110 sample) at 10 K. The slopes at long time ($t > 10$ ns) are -0.75 for the thin layer and -0.57 for the single crystal. The experimental curves are the compilation of the data for different streak camera measurement ranges. Fits by a power law are superimposed on the experimental data (see text).

effects that are cumulative. First, a strong electron-phonon interaction tends to create polarons. Second, the Coulomb interaction between carriers leads to their binding into an exciton. As explained in Ref. [12], the STE in bulk TiO_2 anatase is intrinsic and is made of two different types of carriers. One is a polaron that is strongly bound and localized in the lattice. The other is a carrier weakly bound to the first one. This configuration explains the large emission band: Such a pair of carriers allows the creation of a wide range of configurations that give rise to the distribution of the emission. Since the two carriers are bound into an exciton and spatially close to one another, the width of the distribution is similar for the

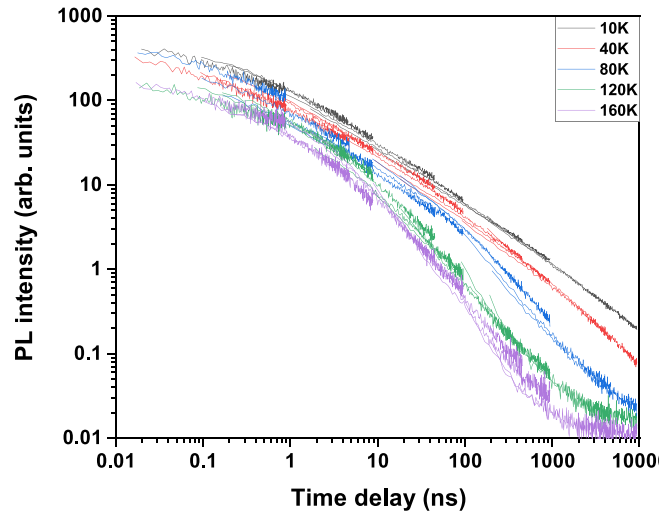

FIG. 7. Dependence on the temperature sample of the time-resolved photoluminescence measured on the magnetron sample. Fits by a power law are superimposed on the experimental data (see text).

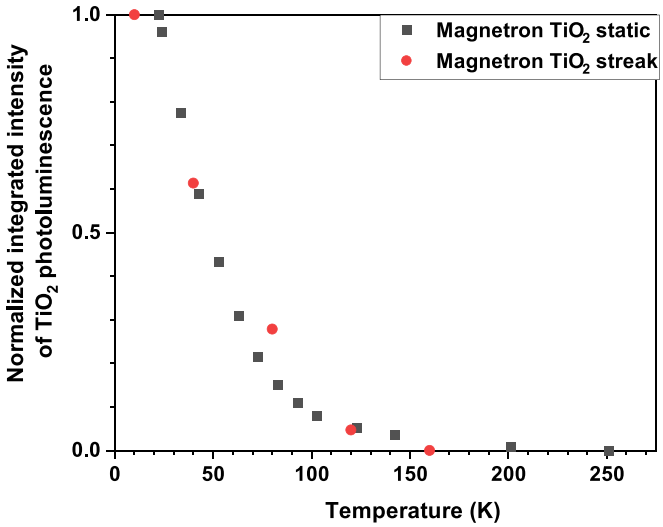

FIG. 8. Comparison of the photoluminescence intensity under cw excitation and of the time integration of emission signal for pulsed excitation as a function of the sample temperature. Both data sets are normalized to their maximum values, around 20 K.

single crystal and the thin film because it is related to local order. Moreover, the detrapping of a weakly bound carrier will explain the quenching of the PL with the temperature, as discussed below.

The main result of our TR-PL measurements is the power-law variation of the photoluminescence with time, which we will now discuss in the framework of this description.

A. Power-law and collision processes

The main feature that is observed from our data is the decay of the emitted intensities, measured on different samples, that presents a power-law dependence with time as evidenced by a straight line at large time delays in a log-log representation. This is a typical feature of a collision process, whose basic equation for the population $n(t)$ describes the interaction between q particles with a nonlinear term:

$$\frac{dn(t)}{dt} = -C\,n^q(t), \tag{1}$$

which gives, for an initial population $n(0)$,

$$n(t) = \frac{n(0)}{(1+(q-1)C\,n^{q-1}(0)\,t)^{\frac{1}{q-1}}}. \tag{2}$$

When $t \gg 1/(C\,n^{q-1}(0))$,

$$n(t) \simeq \left(\frac{1}{(q-1)C\,t}\right)^{\frac{1}{q-1}}. \tag{3}$$

The usual case deals with collisions between two particles ($q = 2$):

$$n(t) = \frac{n(0)}{1+C\,n(0)\,t}. \tag{4}$$

This standard equation of a collision process implies that the recombination probability is simply the product of the probabilities of having the q particles at the same location, as would be the case for the superposition of delocalized particle wave functions. However, we will see later that taking into consideration particle diffusion introduces an exponent to time.

Such a behavior was already described for TiO_2 by Watanabe and co-workers [14,15,24]. They wrote an empirical power law with a general formula [15]:

$$n(t) = \frac{n(0)}{\left(1+\frac{t}{\tau_p}\right)^m}. \tag{5}$$

When plotted in a log-log scale, such a graph shows two features: a plateau at low t values, that ends at a value $t \simeq \tau_p$ giving the turning point of the curve, followed by a linear decay at larger times with a slope given by m. But, comparing with (4), we see that τ_p depends actually on the initial excitation $\tau_p = 1/(C\,n(0))$. Consequently, there is no characteristic time as it depends strongly on the excitation conditions Watanabe *et al.* [14] used *ns* pulses and thus the excitation intensity was high, around 100 $\mu J/cm^2$ at maximum and down to 0.4 $\mu J/cm^2$ with a large number of photo-injected electron-hole pairs per pulse (up to $n \simeq 2\times10^{14}$ photons/cm^2). We use here *fs* pulses, with an energy per pulse of 10 $\mu J/cm^2$ a total number of photons that is significantly lower ($n \simeq 10^{13}$ photons/cm^2) the initial photocarrier density is thus lower and the exponential term used by Watanabe *et al.* [14] to fit the earliest part of the decay is no more visible.

The nonlinear nature of the process makes also difficult the analysis of the emission at very short times. Watanabe and co-workers [14,15,24] proposed an initial exponential decay, with a weight that increases with the excitation intensity. We have seen in our experiments that the instrumental function of the detection apparatus can give rise to such a signal as an artifact in the initial dynamics for a power-law process. Indeed, since the power law describes a process that slows down with time, the major part of the photons are emitted at short times giving a contribution that reproduces the instantaneous response of the detection apparatus.

Our data actually show that the power scale behavior is valid even at the smallest time scale, down to the time resolution of our setup, without the need for involving another process. We can follow that power law from picoseconds up to microseconds, over nearly five orders of magnitude on both the time scale and the intensity scale during the decay. Taking, furthermore, the measurements of Watanabe and co-workers [14,15,24], who observed a power law up to 10 ms, we know that this observation is valid up to this time range.

B. Colliding particles

There are two general cases that give rise to such a decay within photoexcited semiconductors.

The first possibility is to attribute the dynamics we observe to a relaxation process that involves interactions between excitons. This is well known to be a dominant process in the exciton population decay in organic compounds or carbon nanotubes. Their dynamics is given by

$$\frac{dN_X(t)}{dt} = -\frac{N_X(t)}{\tau_X} - A\,N_X^2(t), \tag{6}$$

where N_X is the exciton population. While the dynamics is mainly driven by the second term describing their collisions and proportional to the square of N_X, the recombination and the emitted intensity $I(t)$ are given by the first term, which is proportional to the population. That gives

$$I(t) \propto N_X(t) = \frac{N_X(0)\, e^{-t/\tau_X}}{1 + A\, N_X(0)\, \tau_X (1 - e^{-t/\tau_X})}. \tag{7}$$

When $t \ll \tau_X$, in particular when $A\, N_X(t) \gg 1/\tau_X$, the decay is only driven by the collision term, and one gets

$$I(t) \propto N_X(t) \simeq \frac{N_X(0)}{1 + A\, N_X(0)\, t}. \tag{8}$$

Instead of carriers that are bound into excitons, it is possible to consider a second possibility where the dynamics is governed by collisions between separated electrons (e) and holes (h). They would recombine following a bimolecular process: Both the collision term and the recombination term are proportional to the probability of finding e and h at the same position. In contrast to the previous case, the bimolecular term is responsible for the radiative emission, and the emitted intensity will now be proportional to the square of the carrier population. Denoting $n(t)$ and $p(t)$ as their respective populations, we get

$$\left.\frac{dn(t)}{dt}\right|_{\text{rad}} = \left.\frac{dp(t)}{dt}\right|_{\text{rad}} = -B\, n(t)\, p(t). \tag{9}$$

In the case of an optical excitation, the densities of e and h are equal: $n(t) = p(t)$. The previous equations reduce to (1), and $n(t)$ and $p(t)$ are given by (4). We would obtain thus a decay of the light emission that is given by the bimolecular term that is quadratic as the other collision terms that follow from Coulomb interactions between the carriers. From (4), we would get

$$\begin{aligned} I(t) &= -\frac{dn(t)}{dt} \\ &= C\, n(t)\, p(t) \\ &\propto C \left(\frac{n(0)}{1 + B\, n(0)\, t} \right)^2. \end{aligned} \tag{10}$$

The decays we observe (Fig. 6) at all temperatures are always nicely fitted by power-law decays at any times. For the magnetron sample, the fitted exponents in the power law range between -0.75 at 10 K and -1.4 at 160 K. At low temperature, the absolute value of the exponent is lower than 1, and the process could be interpreted as the recombination of excitons as in Eq. (8) (where the exponent is -1) provided that we consider processes that slow down exciton annihilation (see Sec. IV C). The high-temperature value of -1.4 that we observe gives a decay that is too fast for a process related to collision between excitons. Consequently, this value is only compatible with a process that involves collisions between single carriers: electrons and holes, or, more precisely, the polarons they form with their surrounding phonon cloud.

C. Finite wave packet

The $1/t$ dynamics given at large times by Eq. (8) is faster than the dynamics we observe (Fig. 6), which displays a power dependence down to $1/t^{0.75}$. Indeed, the collision process that we discussed, with a quadratic term $A\, N_X^2(t)$ in Eq. (6), considers excitons that are fully delocalized, with wave functions that cover the entire crystal, such as plane waves in an infinite volume or, more realistically, carrier wave functions in nanocrystals. However, the effect of various collision processes, with phonons or impurities, has to be considered. The wave function becomes then a wave packet which is spatially finite, with a zero limit where they can be described as pointlike particles that have to move to the same location in order to collide. Such a process belongs to the family of diffusion-controlled reactions and can be seen as a diffusion-limited annihilation process [25–29]. For a 1D random diffusion process, the mean distance between two excitons increases as $D\sqrt{t}$, where D is the diffusion constant. The collision process becomes, for pointlike particles, $-A\, N_X^2(t)/D\sqrt{t}$ with C combining the collision efficiency A and the diffusion constant D of the particles. Between those two limiting cases (fully delocalized and pointlike excitons) the size of the exciton wave packet is finite, and with $C = A/D$ we get

$$-C\, \frac{N_X^2(t)}{t^\beta} \tag{11}$$

with $0 \leqslant \beta \leqslant 1/2$. In a 3D space, the diffusion process can be further slowed, as the probability for two particles to reach the same point within a finite time can decrease to zero: The value of the β coefficient can thus become larger than $1/2$.

The general equation we obtain for colliding excitons with finite wave packets is thus

$$\frac{dN_X(t)}{dt} = -\frac{N_X(t)}{\tau_X} - C\, \frac{N_X^2(t)}{t^\beta}, \tag{12}$$

the integration of which results, for $t \ll \tau_X$, in

$$I(t) \propto N_X(t) \simeq \frac{N_X(0)}{1 + \frac{1}{1-\beta}\, C\, N_X(0)\, t^{1-\beta}}. \tag{13}$$

That gives a power law for the intensity that goes between t^{-1} and $t^{-\varepsilon}$ with ε being close to zero. Our experimental data for the magnetron sample when the temperature is 10 K, where $I(t) \simeq t^{-0.8}$, would give a value $\beta \simeq 0.2$.

The same dependency can be found for the case of uncorrelated electrons and holes, which can collide and which will recombine through a bimolecular process. The general equation we obtain for equal densities of electrons and holes is thus

$$\frac{dn(t)}{dt} = -C\, \frac{n^2(t)}{t^\beta}, \tag{14}$$

which gives

$$n(t) = \frac{n(0)}{1 + \frac{1}{1-\beta}\, C\, n(0)\, t^{1-\beta}}. \tag{15}$$

When t is large enough, the emitted intensity is given by

$$I(t) \propto \frac{n^2(t)}{t^\beta} \simeq \left(\frac{1-\beta}{C} \right)^2 \frac{1}{t^{2-\beta}}. \tag{16}$$

That gives a power law for the intensity that goes between t^{-2} and t^{-1}. Even if the nature of the collision process changes

also when it deals with free carriers instead of excitons, considering only the bimolecular recombination as in Eq. (14) fits already the faster decays. Our experimental data for the magnetron sample when the temperature is 160 K and $I(t) \simeq t^{-1.34}$ would give a value $\beta \simeq 0.66$.

D. Self-trapped excitons and polarons

The spectral position and shape of the photoluminescence suggest the usual attribution of this emission to self-trapped excitons (STEs) [30]. Moreover, a process involving their collisions has been stated in previous publications to explain why the decay follows a power law. Identifying the colliding particles as STEs is nevertheless questionable: STEs are strongly localized particles that can hardly move and collide.

However, it is known that STEs can diffuse in the host crystal through a hopping process [30,31]. The decay that we observe at low temperature can therefore be explained by collisions between STEs: When they reach the same site, one of the interacting STEs is annihilated, giving its energy to its partner. The latter is sent to high energy levels, at twice the STE energy of 2.5 eV, from which it can relax down to the STE state within a few picoseconds.

To support this hypothesis, we can consider that, even if STEs can recombine, their radiative lifetime is nevertheless quite long and they are very stable. We can take into account that anatase is an indirect-gap material. Values calculated by Zhu and Gao [32] give, for example, for anatase a direct gap of 4.11 eV at the Γ point of the Brillouin zone. However, there is an indirect gap of 3.57 eV between the minimum of the conduction band (CB) at the Γ point and the maximum of the valence band (VB) at a Δ point. After their photoexcitation, electrons (e) and holes (h) are thus quickly separated in the reciprocal space: Such e-h pairs hardly recombine radiatively and are thus very stable. They will afterwards merge into STEs. This results from strong coupling between the carriers and the lattice that leads to the formation of polarons. Electrons and holes are, on the other side, described by wave packets in the k space that will spread and overlap, as soon as the lattice-carrier interaction localizes them. This allows them to overcome the separation in reciprocal space of the two carriers located at different k points. STEs show a finite recombination probability, as the separation between the two carriers within excitons is strongly reduced into a volume given by the Bohr radius.

E. Increasing temperature

When increasing the sample temperature, the experimental data remain nicely fitted by the power law indicating that the decay is still driven by diffusion-limited collision mechanisms, without any other involved processes. Nevertheless, higher temperatures change the overall process speed, which becomes faster, as shown in Fig. 9 by the exponent we deduce from the fits. Higher absolute values for the negative exponent show that the carriers undergo collisions with higher rates.

Moreover, we observe that the emission intensity decreases with the temperature, as shown in Fig. 8. The signal is time integrated: The total intensity diminishes, following the same law as for the static experiments where we used a cw

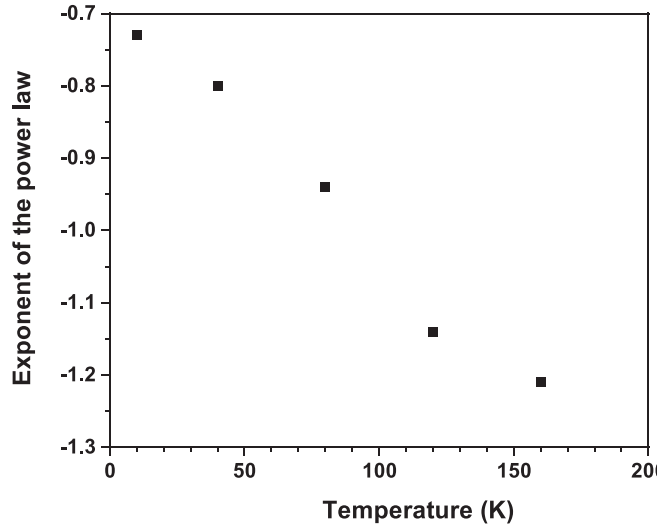

FIG. 9. Exponent of the power law used to fit the experimental data as a function of the sample temperature.

excitation. We have previously proposed [12] that the decrease with temperature of the emitted intensity can be described by a thermally activated process. We expect that STEs are thermally ionized when the temperature is increased and are transformed into separated polarons. We can reasonably estimate that the electron polaron is the lighter particle and can move freely, while the hole polaron shows a higher mass and moves through a hopping process.

The ionization of the STEs into separate electron and hole polarons leads to two changes. First, the interactions that are responsible for the fast dynamics will more and more occur now between polarons, instead of between STEs. Those collisions can expel the carriers from the band extrema and transfer them to trapping states at the crystal surface, where they can be used in redox reactions. Second, their radiative recombination becomes a bimolecular process described by Eqs. (14) and (16), where the carriers have to reach the same point before being annihilated into a photon.

V. CONCLUSION

Our analysis of the time-resolved photoluminescence we measured on anatase TiO_2 samples shows that the decay dynamics can be fit by a power law at any temperature. In light of this information, we unveiled the existence of a collision mechanism that drives the recombination in this material. At low temperature, the photocarriers form self-trapped excitons. Their wave function is spatially finite, and they diffuse by a hopping process inside the crystal. The decrease in the population is driven by interactions between STEs. As the STEs are made of two different carriers, namely, a light electron polaron and a heavier hole polaron, the increase in the temperature can induce the ionization of the STEs. The light electron polaron will thus be able to freely move inside the crystal, while the hole will still diffuse through a hopping process. The collision process between carriers leads to the radiative decay of the carriers and their transport to chemically active sites.

[1] X. Chen and S. Mao, Titanium dioxide nanomaterials: Synthesis, properties, modifications, and applications, Chem. Rev. **107**, 2891 (2007).

[2] M. Grätzel, Photoelectrochemical cells, Nature (London) **414**, 338 (2001).

[3] B. O'Regan and M. Grätzel, A low-cost, high-efficiency solar cell based on dye-sensitized colloidal TiO_2 films, Nature **353**, 737 (1991).

[4] M. Xu, Y. Gao, E. M. Moreno, M. Kunst, M. Muhler, Y. Wang, H. Idriss, and C. Wöll, Photocatalytic activity of bulk TiO_2 anatase and rutile single crystals using infrared absorption spectroscopy, Phys. Rev. Lett. **106**, 138302 (2011).

[5] K. Bourikas, C. Kordulis, and A. Lycourghiotis, Titanium dioxide (anatase and rutile): Surface chemistry, liquid-solid interface chemistry, and scientific synthesis of supported catalysts, Chem. Rev. **114**, 9754 (2014).

[6] L. G. J. De Haart, A. J. de Vries, and G. Blasse, On the photoluminescence of semiconducting titanates applied in photoelectrochemical cells, J. Solid State Chem. **59**, 291 (1985).

[7] R. Leonelli and J. L. Brebner, Time-resolved spectroscopy of the visible emission band in strontium titanate, Phys. Rev. B **33**, 8649 (1986).

[8] H. Tang, H. Berger, P. E. Schmid, and F. Levy, Photoluminescence in TiO_2 anatase single crystals, Solid State Commun. **87**, 847 (1993).

[9] H. Tang, F. Lévy, H. Berger, and P. E. Schmid, Urbach tail of anatase TiO_2, Phys. Rev. B **52**, 7771 (1995).

[10] N. Hosaka, T. Sekiya, and S. Kurita, Excitonic state in anatase TiO_2 single crystal, J. Lumin. **72-74**, 874 (1997).

[11] H. Bieber, P. Gilliot, M. Gallart, N. Keller, V. Keller, S. Bégin-Colin, C. Pighini, and N. Millot, Temperature dependent photoluminescence of photocatalytically active titania powder, Catal. Today **122**, 101 (2007).

[12] M. Gallart, T. Cottineau, B. Hönerlage, V. Keller, N. Keller, and P. Gilliot, Temperature dependent photoluminescence of anatase and rutile TiO_2 single crystals: Polaron and self trapped exciton formation, J. Appl. Phys. **124**, 133104 (2018).

[13] S. Bégin-Colin, A. Gadalla, G. Le Caër, O. Humbert, F. Thomas, O. Barres, F. Villiéras, L. F. Toma, G. Bertrand, O. Zahraa, M. Gallart, B. Hönerlage, and P. Gilliot, On the origin of the decay of the photocatalytic activity of TiO_2 powders ground at high energy, J. Phys. Chem. C **113**, 16589 (2009).

[14] M. Watanabe, S. Sasaki, and T. Hayashi, Time-resolved study of photoluminescence in anatase TiO_2, J. Lumin. **87-89**, 1234 (2000).

[15] M. Watanabe and R. Hayashi, Time-resolved study of self-trapped exciton luminescence in anatase TiO_2 under two-photon excitation, J. Lumin. **112**, 88 (2005).

[16] N. Harada, M. Goto, K. Iijima, H. Sakama, N. Ichikawa, H. Kunugita, and K. Ema, Time-resolved luminescence of TiO_2 powders with different crystal structures, Jpn. J. Appl. Phys. **46**, 4170 (2007).

[17] T. Hashimoto, K. Takahashi, H. Kunugita, H. Sakama, and K. Ema, Dynamics of photo-excited carriers in anatase TiO_2 thin film investigated by pump-probe method, J. Phys.: Conf. Ser. **193**, 012051 (2009).

[18] K. Wakabayashi, Y. Yamaguchi, T. Sekiya, and S. Kurita, Time-resolved luminescence spectra in colorless anatase TiO_2 single crystal, J. Lumin. **112**, 50 (2005).

[19] J. Zhang, X. Chen, Y. Shen, Y. Li, Y. Hu, and J. Chu, Synthesis, surface morphology and photoluminescence properties of anatase iron-doped titanium dioxide nano-crystalline films, Phys. Chem. Chem. Phys. **13**, 13096 (2011).

[20] S. M. Gupta and M. Trpathi, A review of TiO_2 nanoparticles, Chin. Sci. Bull. **56**, 1639 (2011).

[21] J. Schneider, M. Matsuoka, M. Takeuchi, J. Zhang, Y. Horiuchi, M. Anpo, and D. W. Bahnemann, Understanding TiO_2 photocatalysis: Mechanisms and materials, Chem. Rev. **114**, 9919 (2014).

[22] D. K. Pallotti, L. Passoni, P. Maddalena, F. Di Fonzo, and S. Lettieri, Photoluminescence mechanisms in anatase and rutile TiO_2, J. Phys. Chem. C **121**, 9011 (2017).

[23] K. Iijima, M. Goto, S. Enomoto, H. Kunugita, K. Ema, M. Tsukamoto, N. Ichikawa, and H. Sakama, Influence of oxygen vacancies on optical properties of anatase TiO_2 thin films, J. Lumin. **128**, 911 (2008).

[24] M. Watanabe, T. Hayashi, H. Yagasaki, and S. Sasaki, Luminescence process in anatase TiO_2 studied by time-resolved spectroscopy, Int. J. Mod. Phys. B **15**, 3997 (2001).

[25] S. H. Northrup and J. T. Hynes, On the description of reactions in solution, Chem. Phys. Lett. **54**, 244 (1978).

[26] Z. Zhu, J. Crochet, M. S. Arnold, M. C. Hersam, H. Ulbricht, D. Resasco, and T. Hertel, Pump-probe spectroscopy of exciton dynamics in (6,5) carbon nanotubes, J. Phys. Chem. C **111**, 3831 (2007).

[27] A. Srivastava, H. Htoon, V. I. Klimov, and J. Kono, Direct observation of dark excitons in individual carbon nanotubes: Inhomogeneity in the exchange splitting, Phys. Rev. Lett. **101**, 087402 (2008).

[28] Y. Murakami and J. Kono, Nonlinear photoluminescence excitation spectroscopy of carbon nanotubes: Exploring the upper density limit of one-dimensional excitons, Phys. Rev. Lett. **102**, 037401 (2009).

[29] J. Allam, M. T. Sajjad, R. Sutton, K. Litvinenko, Z. Wang, S. Siddique, Q.-H. Yang, W. H. Loh, and T. Brown, Measurement of a reaction-diffusion crossover in exciton-exciton recombination inside carbon nanotubes using femtosecond optical absorption, Phys. Rev. Lett. **111**, 197401 (2013).

[30] K. S. Song and R. Williams, *Self-Trapped Exitons*, 2nd ed. (Springer-Verlag, Berlin, 1993).

[31] K. Tanimura and N. Itoh, The hopping motion of the self-trapped exciton in NaCl, J. Phys. Chem. Solids **42**, 901 (1981).

[32] T. Zhu and S.-P. Gao, The stability, electronic structure and optical property of TiO_2 polymorphs, J. Phys. Chem. C **118**, 11385 (2014).